Letter

Matrix product operator approach to nonequilibrium Floquet steady states

Zihan Cheng[1] and Andrew C. Potter[1,2]
[1]*Department of Physics, University of Texas at Austin, Austin, Texas 78712, USA*
[2]*Department of Physics and Astronomy, and Quantum Matter Institute, University of British Columbia, Vancouver, British Columbia, Canada V6T 1Z1*

(Received 28 July 2022; revised 19 October 2022; accepted 13 December 2022; published 23 December 2022)

We present a numerical method to simulate nonequilibrium Floquet steady states of one-dimensional periodically driven many-body systems coupled to a dissipative bath, based on a matrix product operator ansatz for the Floquet density matrix in frequency space. This method enables access to large systems beyond the reach of exact simulations, while retaining the periodic micromotion information. An excited-state extension of this technique allows computation of the dynamical approach to the steady state. We benchmark our method with a driven-dissipative Ising model and apply it to study the possibility of stabilizing prethermal discrete time-crystalline order by coupling to a cold bath.

DOI: 10.1103/PhysRevB.106.L220307

Controlling quantum systems with time-periodic (Floquet) external driving fields offers a powerful toolkit to engineer interactions, symmetry breaking, and topology that are not present in the undriven system [1]. Floquet driving can also produce *intrinsically nonequilibrium* phenomena such as dynamical phases, particularly time crystals and Floquet topological phases [2,3], with properties that would be impossible in static equilibrium. However, for isolated systems, persistent energy absorption from the external ordinarily produces runaway heating to a featureless state [4,5] that is locally indistinguishable from an infinite temperature ensemble. Thus, to stabilize dynamical phases in closed Floquet systems, one usually considers systems with many-body localization (MBL) [6] that fail to thermalize, or work in a prethermal regime [7–13] where Floquet states can live up to an exponentially long timescale $\tau_{\text{heat}} \sim e^{\Omega/\Lambda}$ in the ratio of driving frequency Ω, to the local bandwidth Λ. Both of these approaches have substantial limitations. First, MBL requires synthesizing strong disorder, and is fundamentally incompatible with many interesting phenomena such as non-Abelian symmetries and anyons [14], Goldstone modes [15], long-range interactions, and (at least as a matter of principle if not practice) in dimensions higher than one [16]. Second, no experimental system is truly isolated from its environment, which restricts MBL-protected order to transient times. Realizing prethermal *quantum* phases requires preparing a low-temperature state of the prethermal Hamiltonian which is typically hard to even calculate, let alone prepare its ground state (e.g., adiabatic state preparation generally fails in Floquet settings [17]).

From experience with solid-state physics, it is natural to look to dissipation from a cold bath to cool a Floquet system close to its prethermal ground state. For fast, weakly heating drives, rigorous bounds on prethermalization [7–13] establish a large separation of timescales between the drive period $\tau = 2\pi/\Omega$, and the heating time τ_{heat}. This suggests an ample range of parameter space to couple the system to a bath weakly enough to avoid disrupting the interesting Floquet dynamics, while cooling towards the prethermal ground state at a rate much higher than the drive-induced heating. On the other hand, coupling a system to a bath can enhance drive-induced heating, by broadening spectral lines in the system to enable off-resonant drive-induced excitations that cause the system to heat [18]. To explore the balance between these competing processes and establish whether dissipation can stabilize dynamical orders in an appropriately designed range of drive, bath, and system-bath coupling parameters, requires a controlled calculation method that can simultaneously treat strong driving, interactions, and open system dynamics.

However, solving the long-time nonequilibrium steady state (NESS) of a generic Floquet-Lindblad equation [19–22] (FLE) is a challenging task, even for one-dimensional systems. Similar to solving the Schrödinger equation, the cost of exact treatment grows exponentially with respect to the system size, but with a *double* exponent due to simulating density matrices rather than pure states. Quantum trajectory sampling methods [23–25] reduce the memory cost, but may incur exponential-in-system-size sampling overheads.

In one dimension (1D), matrix product states (MPS) and operators (MPOs) provide an effective way of representing systems with limited spatial entanglement—a class that includes not only ground states of gapped systems [26] but also thermal mixed states [27]. One class of MPO approaches [28–31], in combination with time-evolving block decimation (TEBD) methods, allows studying the NESS via long-time dynamics. Such real-time approaches can suffer from the long relaxation time to the NESS, for example, in the presence of long-time hydrodynamic tails, and weakly dissipative systems may also feature a rapid growth of entanglement in the transient regime that cannot be captured by a low bond-dimension MPO [32–35], presenting a short-time barrier to accessing the NESS through time evolution.

To overcome these limitations, for time-independent systems, recent works [33,34] directly target an MPO

representation of a NESS that is variationally optimized through density matrix renormalization group (DMRG)-type methods [36], while there are also Floquet DMRGs targeting eigenstates in closed (e.g., MBL) systems [37,38]. In this Letter, we extend this technique to open Floquet systems, dubbed the open-system Floquet DMRG (OFDMRG). The central idea will be to reduce the time-dependent Floquet problem to an effective time-independent one in an extended (frequency) space. Frequency-space methods are widely used in various analytic and numerical approaches to Floquet problems [38,39]. Here, we adapt this representation in a form convenient for performing MPS calculations. Importantly, the method retains information not only about the NESS at stroboscopic times, but also the micromotion within a period, which can be required to observe certain dynamical phases, such as Floquet topological insulators and symmetry-protected topological phases [2]. We benchmark our method with a driven-dissipative Ising model and also use it to explore the dissipative stabilization of a discrete time crystal (DTC) by coupling it to a cold bath.

Frequency-space MPO representation. Consider the evolution of the density matrix $\rho(t)$ of a periodically driven 1D quantum system coupled to a Markovian bath described by the Floquet-Lindblad equation (FLE),

$$\partial_t \rho = \mathcal{L}(t)[\rho] = -i[H(t), \rho] + \sum_\alpha \left(L_\alpha(t)\rho L_\alpha^\dagger(t) - \frac{1}{2}\{L_\alpha^\dagger(t)L_\alpha(t), \rho\} \right), \quad (1)$$

where $H(t+\tau) = H(t)$ and $L_\alpha(t+\tau) = L_\alpha(t)$ are respectively the periodic Hamiltonian and jump operators.

Floquet's theorem enables one to write solutions to the FLE in terms of quasieigenmodes of the Lindbladian $\mathcal{L}(t)$ as $\rho(t) = \sum_n \rho^n e^{-\lambda t} e^{in\Omega t}$, where λ is the (complex) quasieigenvalue and $\Omega = 2\pi/\tau$ is the driving frequency (see Supplemental Material [40] Sec. I). Inserting this expression into Eq. (1) reduces the time-dependent FLE into an effectively time-independent equation, $\hat{\mathcal{L}}[\hat{\rho}] = -\lambda\hat{\rho}$ for extended $\hat{\rho} = \sum_n \rho^n \otimes |n\rangle\rangle$ residing in an enlarged (frequency) space $\mathcal{H}^2 \times \mathbb{Z}$ (intuitively, the extra $\mathbb{Z}$ factor keeps track of how many drive quanta the system has absorbed or released), where the extended Lindbladian is given by

$$\hat{\mathcal{L}}^{nm}[\rho^m] = -in\Omega\rho^n\delta_{nm} - i[H^{n-m}, \rho^m] + \sum_\alpha D_\alpha^{nm}[\rho^m],$$
$$D_\alpha^{nm}[\rho^m] = L_\alpha^{n-k}\rho^m L_\alpha^{\dagger,k-m} - \frac{1}{2}\{L_\alpha^{\dagger,n-k}L_\alpha^{k-m}, \rho^m\}, \quad (2)$$

where H^n and L_α^n are Fourier coefficients of H and L_α with frequency $n\Omega$, respectively, and throughout this Letter repeated Fourier indices are implicitly summed.

We are targeting models with high-frequency drives and weak system-bath couplings to model whether a system can be cooled close to a prethermal ground state. Here, we expect ρ^0 to be approximately thermal, and hence exhibit an area-law operator entanglement [27] permitting efficient representation as an MPO. We further assume that, at high frequencies, the linear potential $-in\Omega$ in frequency space leads to localization near $n = 0$ characterized by a rapid decay of $|\rho^n|/|\rho^0|$ with n (see Supplemental Material [40] Sec. II for a convergence check), so that we can cut off the infinite frequency index

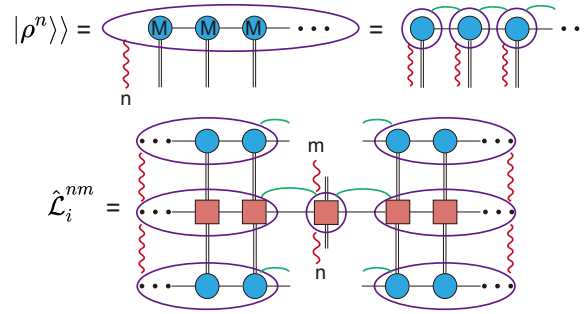

FIG. 1. Graphical representation of vectorized MPOs $|\rho^n\rangle\rangle$ (upper) and effective local Lindbladian $\hat{\mathcal{L}}_i^{nm}$ (lower) in frequency space. Blue circles and black single/double lines respectively represent the tensor and bond/physical indices in the Hilbert space, while the purple circle and red wavy lines represent the tensor and Fourier indices in frequency space. Green lines represent the virtual bonds, where each MPO block is diagonal in the frequency space.

beyond $|n| = N_c$, and that each ρ^n has a low bond-dimension MPO representation $\forall n$. The validity of the assumptions can be checked *a posteriori*. We note that the Fourier index n can be regarded either as a global index, or distributed to each MPO by introducing virtual bonds which formally require each MPS block diagonal in the frequency space, i.e., no interplay between different frequency space sectors (see Fig. 1 for a graphical representation). It is further convenient to vectorize the density matrices $\rho^n \to |\rho^n\rangle\rangle$ using the Choi isomorphism $|\psi\rangle\langle\phi| \to |\psi \otimes \phi\rangle\rangle$, so that we regard the MPO as an MPS with a squared physical dimension,

$$|\rho^n\rangle\rangle = \sum_{\{\mu_i\}} M^n_{\mu_1} \cdots M^n_{\mu_L} |\mu_1 \cdots \mu_L\rangle\rangle, \quad (3)$$

where each M^n is a $d^2 \times \chi \times \chi$ tensor, d is the on-site Hilbert space dimension, $\mu_i \in \{1 \ldots d^2\}$ labels a basis of physical states for the vectorized density matrix, $i = 1 \ldots L$ label sites of the 1D chain, and χ is the bond dimension.

After the vectorization, $\hat{\mathcal{L}}^{nm}$ in Eq. (2) becomes a linear operator acting on $|\rho^m\rangle\rangle$, which can be similarly represented in an MPO form with two Fourier components n, m,

$$\hat{\mathcal{L}}^{nm} = \sum_{\{\mu_i,\nu_i\}} v^L W^{nm}_{\mu_1\nu_1} \cdots W^{nm}_{\mu_N\nu_N} v^R |\mu_1 \cdots \mu_N\rangle\rangle\langle\langle \nu_1 \cdots \nu_N|, \quad (4)$$

where each W^{nm} is a $d^2 \times d^2 \times \chi_O \times \chi_O$ tensor, χ_O are the operator bond dimensions, and $v^{L,R}$ impose boundary conditions.

Open-system Floquet DMRG (OFDMRG). In conventional MPS-DMRG for closed systems, one minimizes the variation energy $\langle\psi|H|\psi\rangle$ for each local MPS tensor, which relies heavily on the Hermiticity of H. A natural generalization [33] to open systems would be to minimize $\langle\langle\rho|\mathcal{L}^\dagger\mathcal{L}|\rho\rangle\rangle$, however, the MPO for $\mathcal{L}^\dagger\mathcal{L}$ has a square of the bond dimension of that for $\mathcal{L}$, adding significant overhead [34]. In an alternative approach [34], instead of variationally searching for the local MPS, one can solve the zero eigenvector for the local effective Lindbladian $\mathcal{L}_i$ obtained by contracting all indices for $\langle\langle\rho|\mathcal{L}|\rho\rangle\rangle$, except those for a single site i, so that sites $j \neq i$ form an environment for site i.

Here, we adapt this approach directly to the frequency-space representation of ρ and $\hat{\mathcal{L}}$, seeking to approximately prepare the NESS satisfying $\hat{\mathcal{L}}_i^{nm}|\rho^m\rangle\rangle = 0$ by sweeping through a sequence of local eigenvalue problems for $M_{\mu_i}^m$ (see Fig. 1), using an implicitly restarted Arnoldi method based non-Hermitian eigensolver implemented in the ARPACK library [41]. Working in frequency space requires imposing additional constraints on the solutions. Physical states satisfy $\mathrm{Tr}\,\rho(t) = \langle\langle\mathbb{I}|\rho(t)\rangle\rangle = 1 \forall t$, which demands $\mathrm{Tr}\,\rho^n = \langle\langle\mathbb{I}|\rho^n\rangle\rangle = \delta_{n0}$, where $|\mathbb{I}\rangle\rangle$ is the maximally mixed state. We enforce this condition by penalizing violations by modifying how the extended Lindbladian acts on vectors as $\hat{\mathcal{L}} \to \hat{\mathcal{L}}'$ with

$$\begin{aligned}\hat{\mathcal{L}}'^{nm}|\rho^m\rangle\rangle =& [\hat{\mathcal{L}}^{nm} - P_0|\mathbb{I}\rangle\rangle\langle\langle\mathbb{I}|(1-\delta_{n0})\delta_{nm}]|\rho^m\rangle\rangle \\ & - P_1 \exp(-|\mathrm{Tr}\,\rho^0|^2/\delta^2)|\rho^n\rangle\rangle, \end{aligned} \tag{5}$$

where P_0, P_1, δ are penalty parameters. In practice, we start with several warm-up sweeps with proper penalty parameters ($P_0 = P_1 = 1000$ and $\delta = 0.01$ in our implementation) to avoid local minima violating the trace constraint, and then remove the penalty for further DMRG sweeping (see Supplemental Material [40] Secs. II and III for a discussion on convergence and positivity of density matrices).

Dynamical approach to the NESS. The MPO-based method can be naturally extended to solve long-lived decaying modes of the Floquet Lindbladian, with $\mathrm{Re}\,\lambda > 0$, by a similar approach to excited-state DMRG [42]. To explore this, we first review some basic properties of the (extended) Lindbladian: (i) The Lindbladian has a biorthonormal basis, where left and right eigenvectors are defined by $\hat{\mathcal{L}}|\rho_\alpha^R\rangle\rangle = \lambda_\alpha|\rho_\alpha^R\rangle\rangle$ and $\hat{\mathcal{L}}^\dagger|\rho_\alpha^L\rangle\rangle = \lambda_\alpha^*|\rho_\alpha^L\rangle\rangle$ and satisfy the orthogonal relations $\langle\langle\rho_\alpha^L|\rho_\beta^R\rangle\rangle = \delta_{\alpha\beta}$. (ii) The corresponding eigvenvalues $\{\lambda_{\alpha=0,1,\ldots}\}$ can be sorted as $0 = \lambda_0 > \mathrm{Re}\,\lambda_1 \geqslant \mathrm{Re}\,\lambda_2 \geqslant \cdots$ (we assume that the zero eigenvalue is not degenerate in the following discussion). In particular, $|\rho_0^L\rangle\rangle = |\mathbb{I}\rangle\rangle$ due to the trace preservation of the Lindblad operator. (iii) The complex eigenvalues must occur in a pair of complex conjugates since when ρ is an eigenvector, $\rho^\dagger$ is also an eigenvector.

Based on the properties of the Lindbladian and in analogy to the Hamiltonian case [42], one can define $\hat{\mathcal{L}}_1 = \hat{\mathcal{L}} - w|\mathbb{I}\rangle\rangle\langle\langle\mathbb{I}|$ ($\hat{\mathcal{L}}_1^\dagger = \hat{\mathcal{L}}^\dagger - w|\rho_{ss}\rangle\rangle\langle\langle\rho_{ss}|$), where w is the penalty energy for the vector not orthogonal to the zeroth left (right) eigenvector. For large enough w, the solved eigenvalue with the largest real part will give the first right (left) eigenvector $|\rho_1^R\rangle\rangle$ ($|\rho_1^L\rangle\rangle$). In principle, this procedure can be done recursively to the nth eigenvector by adding n projectors, however, for the pair of eigenvectors whose eigenvalues are in complex conjugate pairs $\lambda = a \pm ib$, they cannot be distinguished by their real part. Thus, we focus only on the first decaying mode by targeting the largest real part of eigenvalues, which dominates the approach to the steady state at long times.

Benchmark: Driven-dissipative Ising chain. We first benchmark our OFDMRG method in a driven-dissipative Ising model on a length L spin-1/2 chain with Pauli operators $\{X_i, Y_i, Z_i\}$ for sites $i = 1 \ldots L$ with the Hamiltonian

$$H(t) = \sum_i [p(t)(-JZ_iZ_{i+1} + hZ_i) + q(t)gX_i], \tag{6}$$

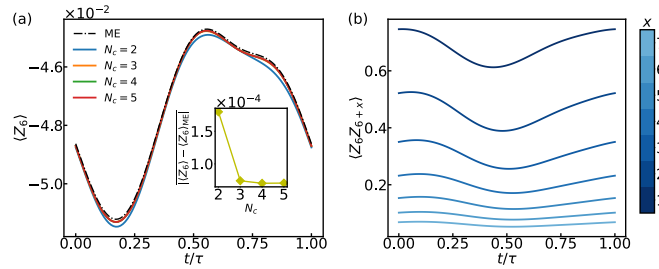

FIG. 2. NESS of driven-dissipative Ising chain with $(J, h, g, \gamma, \omega) = (1.0, 0.5, 1.0, 1.0, 5.0)$. (a) Time-dependent expectation values of magnetization $\langle Z_6\rangle$ for a system size $L = 11$, with $\chi = 36$, compared with the master equation evolution result. The period-averaged error (inset) decays rapidly with N_c to the numerical accuracy of the eigensolver. (b) Spatial correlations $\langle Z_6 Z_{6+x}\rangle$ for a larger chain with $L = 21$, using $(N_c, \chi) = (4, 20)$.

where $p(t) = (1 - \sin\omega t)/2$, $q(t) = (1 + \sin\omega t)/2$, and time-independent majority-rule jump operators

$$\begin{aligned} L_i = \sqrt{\gamma}[&2|\uparrow\uparrow\uparrow\rangle\langle\uparrow\downarrow\uparrow| + |\uparrow\uparrow\downarrow\rangle\langle\uparrow\downarrow\downarrow| \\ &+ |\uparrow\downarrow\downarrow\rangle\langle\uparrow\uparrow\downarrow| + (\uparrow\leftrightarrow\downarrow)]. \end{aligned} \tag{7}$$

To compare our method with the exact evolution of the Lindblad master equation implemented in QUTIP [43], we simulate a chain with an array length $L = 11$. We find excellent convergence in the central magnetization $\langle Z_6\rangle$ to the exact solution with increasing frequency-space cutoff N_c, achieving a residual error $\sim 10^{-4}$ for $N_c \sim 5$ that is consistent with the residual error in the zero-eigenvalue solver of OFDMRG and the order of magnitude of Schmidt components at the bond-dimension cutoff (see Supplemental Material [40] Sec. II). The OFDMRG method also extends straightforwardly to larger systems with polynomial-in-L scaling. For example, in Fig. 2 we show spatial correlations for a size $L = 21$, which would require enormous computational resources to compute exactly.

Dissipatively stabilizing a discrete time crystal (DTC). Having benchmarked the performance of the OFDMRG approach, we now turn to the question of whether a prethermal dynamical phase can be stabilized by coupling to a cold bath. As an example, we study a model for a prethermal DTC model [11] coupled to a thermal bath. For the system part, we consider one-dimensional Ising model driven by periodic π pulses with generic perturbation breaking the $\mathbb{Z}_2$ symmetry, which serves as a prototypical model for the prethermal DTC [11]

$$H(t) = \sum_i \left[\frac{\pi}{2}\sum_n \delta(t - n\tau)X_i - JZ_iZ_{i+1} + hZ_i f(t) + gX_i\right], \tag{8}$$

where $f(t) = (1 - \cos\Omega t)$. Various disordered and/or long-range interacting incarnations of this Hamiltonian have been studied in previous theoretical studies and implemented experimentally in a variety of systems [2,3] to study MBL and prethermal mechanisms for stabilizing DTC order in (approximately) closed systems.

Here, we introduce dissipation by coupling each spin, $\sqrt{\gamma}X_i \otimes B_i$, where γ is the coupling strength and B_i are bath operators corresponding to a separate ohmic bath with a

spectral function $J(\varepsilon) = \frac{\varepsilon}{\varepsilon_0} e^{-|\varepsilon|/\omega_c}/(1 - e^{-\beta\varepsilon})$, where $\beta = 1/T$ is the inverse temperature of the bath, ε_0 is a characteristic energy scale, and ω_c is the local bandwidth of the bath, which will play an important role in controlling the steady state [44]. We compute the effective time-dependent jump operators for this model using a Born-Markov approximation (see Supplemental Material [40] Sec. IV), and then truncate these to a finite range of $(2r + 1)$ sites to incorporate into the OFDMRG procedure.

The singular δ train has an unbounded Fourier spectrum, which would be long range in frequency space. However, for models with smooth $f(t)$ satisfying $f(0) = 0$, we can cure this by transforming them into a rotating frame of the δ-function X_π pulses. In the rotating frame the periodicity is doubled to 2τ, but there is a dynamical symmetry: $H(t + \tau) = XH(t)X$ with $X = \prod_i X_i$. In the DTC phase [2,3], this dynamical symmetry is spontaneously broken, resulting in persistent period-doubled oscillations, and manifesting in long-range mutual information between distant spins [45]. However, unlike the long-range interacting prethermal DTC model realized recently in trapped-ion experiments [46], such spontaneous symmetry breaking is forbidden in any short-range interacting 1D system that thermalizes to a finite temperature. Instead, one expects the length scales and timescales for these signatures to diverge if the system is successfully cooled to a prethermal ground state. The criterion of cooling near the prethermal ground is also required to realize dynamical Floquet topological phases (in any dimension), whose properties rely crucially on quantum coherence and entanglement.

Our goal is to assess whether and under what conditions the resulting NESS resembles a low-temperature Floquet-Gibbs state with extended range DTC correlations. To this end, we compute (i) the NESS entropy $S_{\rm ss} = -{\rm Tr}(\rho_{\rm ss} \log \rho_{\rm ss})$, and (ii) the NESS DTC spatial correlation length ξ defined by fitting the averaged correlation function $\overline{\langle Z_{j+x} Z_j \rangle}$ to the form $e^{-x/\xi}$ [shown in Fig. 3(b)]. The NESS results are compared to properties of a thermal state $\rho_{\rm thermal} = \frac{1}{\mathcal{Z}} e^{-\beta D}$, where $D = \sum_i [-JZ_iZ_{i+1} + g(1 - 8ch^2/\Omega^2)X_i]$ with some constant c from $f(t)$ is the effective Floquet Hamiltonian obtained by performing a high-frequency (van Vleck) expansion to the second order. By comparing the system entropy $S_{\rm ss}$ to the thermal entropy of D, we can extract an effective inverse temperature $\beta_{\rm eff} = 1/T_{\rm eff}$ [shown in Fig. 3(a)]. D takes the form of a transverse-field Ising model with an ordered ground state, and the characteristic energy scale to make a local spin-flip excitation of D is $4J$, which results in enhanced drive-induced heating when $\Omega/2 \approx 4J$, and hence enhanced $T_{\rm eff}$. We also compare results to solutions to an approximate Floquet rate equation (FRE) [22,47,48] (for $L = 11$) obtained from a Fermi-Golden rule treatment bath-induced transition rates between eigenstates of the effective system Hamiltonian D in a rotating frame, which neglects off-diagonal coherences in the system density matrix (see Supplemental Material [40] Sec. V). As the driving frequency increases beyond $8J$, this heating is suppressed, and the system's $\beta_{\rm eff}$ asymptotes to that of the bath (note that simulating colder temperatures requires keeping a larger spatial extent r to the *ab initio* computed jump operators), and ξ increases towards the thermal correlation length of $\rho_{\rm thermal}$ at the bath temperature. Importantly, the Floquet-Gibbs state arises only when the local bath bandwidth satisfies $\omega_c \ll |\frac{\Omega}{2} - 4J|$, so that bath-assisted drive-induced heat absorption processes are suppressed (see Supplemental Material [40] Secs. V and VI).

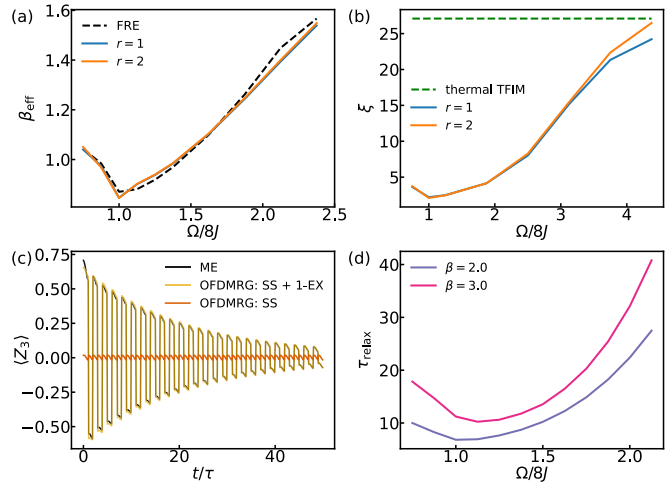

FIG. 3. OFDMRG for the dissipative DTC model Eq. (8) for $J = 1$, $h = 0.5$, $\omega_c = 2$, and unless otherwise specified, $\beta = 2$ and $r = 2$. (a) Comparison between the effective temperature $\beta_{\rm eff}$ of the dissipative DTC model calculated by the OFDMRG method and that from solving the Floquet rate equation (FRE), with $L = 11$, $g = 0.05$, $\gamma = 0.2$, and $(N_c, \chi) = (1, 16)$. (b) Correlation lengths ξ of the dissipative DTC model for $L = 31$, $g = 0.05$, $\gamma = 0.2$, and $(N_c, \chi) = (1, 8)$. The correlation length for a thermal state of the transverse-field Ising model (TFIM) with $\beta = 2$ is given as a reference. (c) Comparison between the transient dynamics of $\langle Z_3 \rangle$ calculated by the OFDMRG method and by the exact evolution of the master equation (ME) for $L = 5$, $g = 0.2$, $\gamma = 2$, $\beta = 5$, high frequency ($\Omega = 10$), and $(N_c, \chi) = (2, 16)$. (d) Relaxation time of the dissipative DTC model for $L = 21$, $g = 0.2$, $\gamma = 2$, and $(N_c, \chi) = (1, 16)$.

We further explore the long-time DTC dynamics, through an asymptotic decay rate $\tau_{\rm relax} = -({\rm Re}\,\lambda_1)^{-1}$ of period doubled oscillations obtained by computing the first excited eigenstate $|\rho_1\rangle\!\rangle$, as well as the explicit dynamics of $\langle Z_j(t) \rangle$ for $|\rho(t)\rangle\!\rangle = |\rho_{\rm ss}\rangle\!\rangle + e^{-\lambda_1 t} \langle\!\langle \rho_I | \rho_1 \rangle\!\rangle |\rho_1\rangle\!\rangle$, which captures the long-time dynamics from an initial product state: $\rho_I = \prod_i [\sin\frac{\pi}{8}|\uparrow\rangle + \cos(\frac{\pi}{8})|\downarrow\rangle][\sin\frac{\pi}{8}\langle\uparrow| + \cos(\frac{\pi}{8})\langle\downarrow|]$. As shown in Fig. 3(c), the dynamical results are compared against exact master equation simulations (for $L = 5$, close to the limit of a single workstation). We observe quantitative agreement between the time-dependent dynamics of the excited-state OFDMRG method with the master equation simulations, confirming that the long-time dynamics is indeed dominated by the first decaying mode. Further, in Fig. 3(d), we observe that the DTC timescale increases with driving frequency Ω (for $\Omega/2 > 4J$), asymptoting to a finite timescale that increases as the bath is cooled.

Discussion and outlook. These results confirm the expectation that there is a parameter regime of large driving frequency ($\Omega \gg 8J$), moderate bath bandwidth ($\omega_c \ll |\frac{\Omega}{2} - 4J|$), and moderately weak system-bath coupling ($e^{-J/\Omega} \ll \gamma \ll J$) where coupling the prethermal DTC model to a bath successfully produces a Floquet-Gibbs-like state with temperature close to that of the bath (see Supplemental Material [40]

Secs. V and VI). Further, the OFDMRG method successfully captures this behavior in system sizes that greatly exceed those accessible by exact master equation simulations (here, we simulated up to $L = 31$ on a single computer, which would be limited to $L \lesssim 6$ for exact computation).

We expect this technique to be useful in designing experimental realizations of dissipatively stabilized dynamical phases in solid-state devices and atomic quantum simulators. The OFDMRG also permits a controlled means to assess the validity of various approximation methods such as Floquet rate equations and truncated Wigner approximation methods [49,50] which could potentially be used beyond 1D. Natural future targets for extending the OFDMRG method include studying NESS of quasiperiodically driven systems [51–53] (with multiple frequency-space directions), and incorporating non-Markovian effects [54,55].

Acknowledgments. We thank Brayden Ware and Romain Vasseur for insightful discussions. This work was supported by NSF DMR-1653007 and the Alfred P. Sloan Foundation through a Sloan Research Fellowship (A.C.P.).

[1] T. Oka and S. Kitamura, Floquet engineering of quantum materials, Annu. Rev. Condens. Matter Phys. **10**, 387 (2019).
[2] F. Harper, R. Roy, M. S. Rudner, and S. L. Sondhi, Topology and broken symmetry in Floquet systems, Annu. Rev. Condens. Matter Phys. **11**, 345 (2020).
[3] D. V. Else, C. Monroe, C. Nayak, and N. Y. Yao, Discrete time crystals, Annu. Rev. Condens. Matter Phys. **11**, 467 (2020).
[4] L. D'Alessio and M. Rigol, Long-time Behavior of Isolated Periodically Driven Interacting Lattice Systems, Phys. Rev. X **4**, 041048 (2014).
[5] A. Lazarides, A. Das, and R. Moessner, Equilibrium states of generic quantum systems subject to periodic driving, Phys. Rev. E **90**, 012110 (2014).
[6] A. Lazarides, A. Das, and R. Moessner, Fate of Many-Body Localization Under Periodic Driving, Phys. Rev. Lett. **115**, 030402 (2015).
[7] D. A. Abanin, W. De Roeck, and F. Huveneers, Exponentially Slow Heating in Periodically Driven Many-Body Systems, Phys. Rev. Lett. **115**, 256803 (2015).
[8] D. A. Abanin, W. De Roeck, W. W. Ho, and F. Huveneers, Effective Hamiltonians, prethermalization, and slow energy absorption in periodically driven many-body systems, Phys. Rev. B **95**, 014112 (2017).
[9] D. Abanin, W. De Roeck, W. W. Ho, and F. Huveneers, A rigorous theory of many-body prethermalization for periodically friven and closed quantum systems, Commun. Math. Phys. **354**, 809 (2017).
[10] M. Bukov, L. D'Alessio, and A. Polkovnikov, Universal high-frequency behavior of periodically driven systems: From dynamical stabilization to Floquet engineering, Adv. Phys. **64**, 139 (2015).
[11] D. V. Else, B. Bauer, and C. Nayak, Prethermal Phases of Matter Protected by Time-Translation Symmetry, Phys. Rev. X **7**, 011026 (2017).
[12] A. Eckardt and E. Anisimovas, High-frequency approximation for periodically driven quantum systems from a Floquet-space perspective, New J. Phys. **17**, 093039 (2015).
[13] K. Mizuta, K. Takasan, and N. Kawakami, High-frequency expansion for Floquet prethermal phases with emergent symmetries: Application to time crystals and Floquet engineering, Phys. Rev. B **100**, 020301(R) (2019).
[14] A. C. Potter and R. Vasseur, Symmetry constraints on many-body localization, Phys. Rev. B **94**, 224206 (2016).
[15] S. Banerjee and E. Altman, Variable-Range Hopping through Marginally Localized Phonons, Phys. Rev. Lett. **116**, 116601 (2016).
[16] W. De Roeck and F. Huveneers, Stability and instability towards delocalization in many-body localization systems, Phys. Rev. B **95**, 155129 (2017).
[17] P. Weinberg, M. Bukov, L. D'Alessio, A. Polkovnikov, S. Vajna, and M. Kolodrubetz, Adiabatic perturbation theory and geometry of periodically-driven systems, Phys. Rep. **688**, 1 (2017).
[18] M. S. Rudner and N. H. Lindner, Band structure engineering and non-equilibrium dynamics in Floquet topological insulators, Nat. Rev. Phys. **2**, 229 (2020).
[19] F. Haddadfarshi, J. Cui, and F. Mintert, Completely Positive Approximate Solutions of Driven Open Quantum Systems, Phys. Rev. Lett. **114**, 130402 (2015).
[20] C. M. Dai, Z. C. Shi, and X. X. Yi, Floquet theorem with open systems and its applications, Phys. Rev. A **93**, 032121 (2016).
[21] T. N. Ikeda and M. Sato, General description for nonequilibrium steady states in periodically driven dissipative quantum systems, Sci. Adv. **6**, eabb4019 (2020).
[22] T. Ikeda, K. Chinzei, and M. Sato, Nonequilibrium steady states in the Floquet-Lindblad systems: van Vleck's high-frequency expansion approach, SciPost Phys. Core **4**, 033 (2021).
[23] K. Mølmer, Y. Castin, and J. Dalibard, Monte Carlo wavefunction method in quantum optics, J. Opt. Soc. Am. B **10**, 524 (1993).
[24] J. Dalibard, Y. Castin, and K. Mølmer, Wave-function approach to dissipative processes in quantum optics, Phys. Rev. Lett. **68**, 580 (1992).
[25] R. Dum, P. Zoller, and H. Ritsch, Monte Carlo simulation of the atomic master equation for spontaneous emission, Phys. Rev. A **45**, 4879 (1992).
[26] U. Schollwöck, The density-matrix renormalization group, Rev. Mod. Phys. **77**, 259 (2005).
[27] M. M. Wolf, F. Verstraete, M. B. Hastings, and J. I. Cirac, Area Laws in Quantum Systems: Mutual Information and Correlations, Phys. Rev. Lett. **100**, 070502 (2008).
[28] F. Verstraete, J. J. García-Ripoll, and J. I. Cirac, Matrix Product Density Operators: Simulation of Finite-Temperature and Dissipative Systems, Phys. Rev. Lett. **93**, 207204 (2004).
[29] M. Zwolak and G. Vidal, Mixed-State Dynamics in One-Dimensional Quantum Lattice Systems: A Time-Dependent Superoperator Renormalization Algorithm, Phys. Rev. Lett. **93**, 207205 (2004).
[30] G. Vidal, Efficient Simulation of One-Dimensional Quantum Many-Body Systems, Phys. Rev. Lett. **93**, 040502 (2004).

[31] S. R. White and A. E. Feiguin, Real-Time Evolution Using the Density Matrix Renormalization Group, Phys. Rev. Lett. **93**, 076401 (2004).
[32] L. Bonnes and A. M. LÃ¤uchli, Superoperators vs. trajectories for matrix product state simulations of open quantum system: A case study, arXiv:1411.4831.
[33] J. Cui, J. I. Cirac, and M. C. Bañuls, Variational Matrix Product Operators for the Steady State of Dissipative Quantum Systems, Phys. Rev. Lett. **114**, 220601 (2015).
[34] E. Mascarenhas, H. Flayac, and V. Savona, Matrix-product-operator approach to the nonequilibrium steady state of driven-dissipative quantum arrays, Phys. Rev. A **92**, 022116 (2015).
[35] H. Weimer, A. Kshetrimayum, and R. Orús, Simulation methods for open quantum many-body systems, Rev. Mod. Phys. **93**, 015008 (2021).
[36] S. R. White, Density matrix formulation for quantum renormalization groups, Phys. Rev. Lett. **69**, 2863 (1992).
[37] C. Zhang, F. Pollmann, S. L. Sondhi, and R. Moessner, Density-matrix renormalization group study of many-body localization in floquet eigenstates, Ann. Phys. **529**, 1600294 (2017).
[38] S. Sahoo, I. Schneider, and S. Eggert, Periodically driven many-body systems: A Floquet density matrix renormalization group study, arXiv:1906.00004.
[39] M. S. Rudner and N. H. Lindner, The Floquet engineer's handbook, arXiv:2003.08252.
[40] See Supplemental Material at http://link.aps.org/supplemental/10.1103/PhysRevB.106.L220307 for the Floquet theorem for open systems, implementation details of OFDMRG, convergence, and positivity check, derivation of jump operators from the microscopic model and their MPO construction, the Floquet rate equation, and conditions for Floquet-Gibbs states, which includes Refs. [56–63].
[41] http://www.caam.rice.edu/software/ARPACK/.
[42] E. M. Stoudenmire and S. R. White, Studying two-dimensional systems with the density matrix renormalization group, Annu. Rev. Condens. Matter Phys. **3**, 111 (2012).
[43] J. R. Johansson, P. D. Nation, and F. Nori, QuTiP 2: A Python framework for the dynamics of open quantum systems, Comput. Phys. Commun. **184**, 1234 (2013).
[44] K. I. Seetharam, C.-E. Bardyn, N. H. Lindner, M. S. Rudner, and G. Refael, Controlled Population of Floquet-Bloch States via Coupling to Bose and Fermi Baths, Phys. Rev. X **5**, 041050 (2015).
[45] D. V. Else, B. Bauer, and C. Nayak, Floquet Time Crystals, Phys. Rev. Lett. **117**, 090402 (2016).
[46] A. Kyprianidis, F. Machado, W. Morong, P. Becker, K. S. Collins, D. V. Else, L. Feng, P. W. Hess, C. Nayak, G. Pagano *et al.*, Observation of a prethermal discrete time crystal, Science **372**, 1192 (2021).
[47] T. Shirai and T. Mori, Thermalization in open many-body systems based on eigenstate thermalization hypothesis, Phys. Rev. E **101**, 042116 (2020).
[48] T. Mori, Floquet states in open quantum systems, arXiv:2203.16358 [Annu. Rev. Condens. Matter Phys. (to be published)].
[49] I. Carusotto and C. Ciuti, Spontaneous microcavity-polariton coherence across the parametric threshold: Quantum Monte Carlo studies, Phys. Rev. B **72**, 125335 (2005).
[50] V. P. Singh and H. Weimer, Driven-Dissipative Criticality within the Discrete Truncated Wigner Approximation, Phys. Rev. Lett. **128**, 200602 (2022).
[51] P. T. Dumitrescu, R. Vasseur, and A. C. Potter, Logarithmically Slow Relaxation in Quasiperiodically Driven Random Spin Chains, Phys. Rev. Lett. **120**, 070602 (2018).
[52] D. V. Else, W. W. Ho, and P. T. Dumitrescu, Long-Lived Interacting Phases of Matter Protected by Multiple Time-Translation Symmetries in Quasiperiodically Driven Systems, Phys. Rev. X **10**, 021032 (2020).
[53] A. J. Friedman, B. Ware, R. Vasseur, and A. C. Potter, Topological edge modes without symmetry in quasiperiodically driven spin chains, Phys. Rev. B **105**, 115117 (2022).
[54] K. Mizuta, K. Takasan, and N. Kawakami, Breakdown of Markovianity by interactions in stroboscopic Floquet-Lindblad dynamics under high-frequency drive, Phys. Rev. A **103**, L020202 (2021).
[55] A. Schnell, S. Denisov, and A. Eckardt, High-frequency expansions for time-periodic Lindblad generators, Phys. Rev. B **104**, 165414 (2021).
[56] A. H. Werner, D. Jaschke, P. Silvi, M. Kliesch, T. Calarco, J. Eisert, and S. Montangero, Positive Tensor Network Approach for Simulating Open Quantum Many-Body Systems, Phys. Rev. Lett. **116**, 237201 (2016).
[57] H.-P. Breuer and F. Petruccione, *The Theory of Open Quantum Systems* (Clarendon, Oxford, U.K., 2002).
[58] F. Nathan and M. S. Rudner, Universal Lindblad equation for open quantum systems, Phys. Rev. B **102**, 115109 (2020).
[59] E. Mozgunov and D. Lidar, Completely positive master equation for arbitrary driving and small level spacing, Quantum **4**, 227 (2020).
[60] D. Tupkary, A. Dhar, M. Kulkarni, and A. Purkayastha, Fundamental limitations in Lindblad descriptions of systems weakly coupled to baths, Phys. Rev. A **105**, 032208 (2022).
[61] F. Nathan and M. S. Rudner, High accuracy steady states obtained from the universal Lindblad equation, arXiv:2206.02917.
[62] Z. Gong and R. Hamazaki, Bounds in nonequilibrium quantum dynamics, Int. J. Mod. Phys. B **36**, 2230007 (2022).
[63] T. Shirai, J. Thingna, T. Mori, S. Denisov, P. Hänggi, and S. Miyashita, Effective Floquet–Gibbs states for dissipative quantum systems, New J. Phys. **18**, 053008 (2016).